CrossMark

Development of transparent conducting palladium and hydrogen-codoped cadmium oxide thin films

A. A. Dakhel[1]

Abstract Cadmium oxide is a transparent conducting oxide (TCO) material with versatile applications, many of which are linked to either light transparency in the NIR spectral range in addition to unique electrical conductivity. Doping is a known approach to influence those optoelectrical properties in order to bring them into a desired choice. In the present work, hydrogenated (annealed in hydrogen atmosphere) cadmium oxide (CdO) thin films doped with different amounts of palladium (Pd) ions were deposited on glass and silicon wafer substrates by physical vapour deposition method. The films were characterized by X-ray diffraction, optical absorption spectroscopy, and dc-electrical measurements. The obtained results show notable improvements in the conductivity, mobility, and carrier concentration of host CdO. Hydrogenated CdO film doped with 15 wt% Pd shows utmost enhancement in mobility (32.02 cm^2/Vs), conductivity (4.6948 × 10^3 S/cm) and carrier concentration (9.16 × 10^{20} cm^{-3}). This suggests the possibility of using hydrogenated Pd-doped CdO films in different TCO field of applications.

1 Introduction

The optoelectronic properties of transparent conducting oxides (TCOs) like ZnO, CdO, SnO$_2$, In$_2$O$_3$, etc. stand on their degenerate semiconducting and unique optical properties. Donor states in nonstoichiometric TCOs arising from metallic ion interstitials and oxygen vacancies give rise to an impurity band grows and merges with the conduction band [1]. Cadmium oxide (CdO), the material of the present study, has n-type semiconducting behavior with relatively low electrical resistivity (10^{-2}–10^{-4} Ω cm) and good transparency especially in the near infrared (NIR) spectral region with a direct bandgap of $\sim$2.2–2.7 eV [2–4]. CdO crystallizes in a cubic structure of space group Fm-3 m of 6-coordination with a lattice constant of 0.4695 nm [5]. CdO has many optoelectronic applications in solar cells, smart windows, and in many other applications [2, 3, 6, 7]. The fundamental optoelectronic properties of CdO could be controlled by doping with different foreign metallic ions such as Al [8], In, Y [1], Sc [9], Fe [10], Sm [11], Sn [6], etc. Furthermore, doping can create exotic properties, such as magnetic, optical, optoelectronic, etc. that would diverse the framework of TCO-CdO applications. Experimentally, it was established that, doping of CdO with metallic ions of smaller size compared to Cd^{2+} (the ionic radius of Cd^{2+} is 0.095 nm [12]) like Ge, W, etc. [13, 14] could improve their conduction parameters [15]. Therefore, doping of CdO with Pd^{2+} ions of radius 0.086 nm (VI-coordination) [12] is expected to improve the conduction parameters of a host CdO. On other hand, Pd is known to posses high catalytic effect for H$_2$ molecules dissociation [16, 17]. Thus the present work deals with catalytic effect [18, 19] that takes place inside the crystalline structure of CdO. Therefore, it is possible to expect that annealing of Pd-doped CdO samples in H$_2$ atmosphere (hydrogenation) could improve the conduction parameters of host CdO that was planned to study in the present work. It should be mentioned that doping of CdO by any means with Pd ions was surprisingly not investigated yet, although such doping was conducted for other TCO's like ZnO [20], SnO$_2$ [21], and In$_2$O$_3$ [22].

✉ A. A. Dakhel
adakhil@uob.edu.bh

[1] Department of Physics, College of Science, University of Bahrain, P.O. Box 32038, Zallaq, Kingdom of Bahrain

The present work reports the effect of Pd doping on the structural, electrical, and optical properties of CdO. It will be seen that the hydrogenation of Pd-doped CdO is efficient to obtain high mobility and conductivity comparing to other types of dopants and could be used for technical applications based on its NIR-TCO characteristics.

2 Experimental details

Several sets of thin films of CdO incorporated with different amounts of palladium ions were prepared. Therefore, the starting materials were pure Pd and CdO (from Fisher sci. company/USA and Fluka A.G./Germany, respectively). The substrates were ultrasonically clean glass slides held in a vacuum chamber of residual oxygen atmosphere of about 1.3×10^{-3} Pa. The alternate (layer-by-layer) vacuum thermal evaporation (vapor deposition) by using alumina baskets (Midwest tungsten service, USA) was used to deposit the starting materials on the substrates. Then, the as-grown films were flash annealed in air at 400 °C for 1 h keeping samples inside the closed furnace for natural cooling to the room temperature. All the samples were prepared in almost the same conditions including the reference pure CdO film. The evaporated masses were controlled with a piezoelectric microbalance crystal sensor of a Philips FTM5 thickness monitor fixed close to the substrate. The final film thicknesses were measured after annealing by an MP100-M spectrometer (Mission Peak Optics Inc., USA), to be in the range 0.10–0.25 μm. The weight ratio of Pd to Cd of the prepared samples were estimated to be $\sim 3, 6, 15$ and 20% and the samples were labeled as S1, S2, S3, and S4, respectively. The structure of the prepared films were studied with X-ray diffraction (XRD) method using a Philips PW 1710 θ–2θ system of a Cu K_α radiation (0.15406 nm) and a step of 0.02°. The normal spectral optical transmittance T(λ) were measured in the spectral range 250–800 nm with a Shimadzu UV-3600 double beam spectrophotometer. The dc electrical parameters (resistivity-ρ, mobility-μ_{el}, and carrier concentration-N_{el}) were measured by Van der Pauw technique at room temperature with aluminum spot contacts in a magnetic field of about 1 T and using a Keithley 195A digital multimeter and a Keithley 225 current source. It should be mentioned that the contact Al/CdO resistance could be neglected in the present case as long as the carrier concentration is larger than 10^{19} cm^{-3} [23].

3 Results and discussion

3.1 Structure analyses

Figure 1a shows the XRD patterns of pure and Pd-doped CdO films. It reveals that all the prepared films are polycrystalline in nature. The peaks were indexed according the standard CdO JCPDS data [5]. The growth of CdO film in the present work was in usual [111] energetically preferred orientation. However, the [111] preferred orientation growth of host CdO film was enhanced with Pd doping towards the total [111] orientation. Identical observation was previously found in case of doping of CdO films with metallic dopants Fe and Cr [10, 24]. The film's orientation growth could be studied through a texture coefficient, TC$_{(hkl)}$ [25];

$$TC_{(hkl)} = \left[n\, I(hkl)/I_0(hkl) \right] \Big/ \left[\sum I'(h'k'l')/I_0(h'k'l') \right]$$

(1)

where I(hkl) is the intensity of (hkl) reflection from a certain film sample and I_0(hkl) is the intensity of that reflection as registered for a standard randomly oriented polycrystalline CdO powder quoted from Ref [5]. The sum
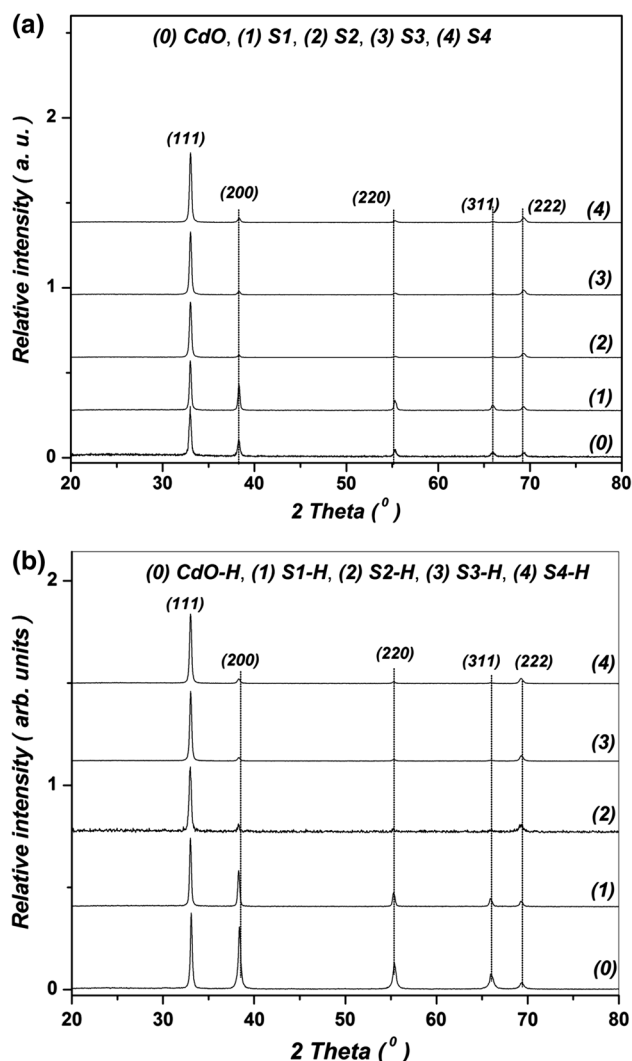

Fig. 1 **a** XRD patterns of undoped and Pd-doped films. **b** XRD patterns of hydrogenated undoped and Pd-doped films

in the above equation runs over the total number (n) of the recorded reflections appeared in the XRD pattern of the present investigation, i.e. (111), (200), (220), and (311) reflections. Therefore, the highest value of $TC_{(hkl)}$ in the present case is 4 for a singly oriented film and is 1 for a randomly oriented one. The calculated values of TCs of [111] direction are given in Table 1, which show that Pd doping increased the value of $TC_{(111)}$ up to ~ 4. It can be seen that with doping level >6%, the films become almost totally [111] oriented. The $TC_{(111)}$ might also be used to measure the film crystallinity and thus it has effects on the electrical conduction properties. The clear effect of Pd incorporation on CdO film growth orientation should refer to a substitutional doping of Pd ions in the crystalline structure of CdO. However, Fig. 1a reveals that doping of Pd ions did not modify the ordinary cubic crystalline structure of host CdO. Furthermore, the XRD patterns of Pd-doped CdO show absence of diffraction peaks arising from pure, oxide, or any Pd related phases, which confirms the doping effect of Pd ions in the crystalline lattice structure of CdO.

Generally, the incorporation of Pd ions in host CdO includes substitution of Cd^{2+} ions by Pd^{2+} ions i.e. forming of substitutional solid solution (SSS), occupation of crystalline point defects and interstitial locations, and accumulation on the crystallite and grain boundaries (CBs and GBs). As long as the % difference of ionic radii of Pd^{2+} and Cd^{2+} ions is $\sim 9\%$, then the ionic doping by substitution of Pd^{2+} ions for structural Cd^{2+} ions would not strongly disturb the crystalline structure of host CdO, according to Hume–Rothery rules [26] and, thus, the formation of SSS is most likely to happen. In addition, substitution of Pd ions of +2-oxidation state would not change the electrostatic neutrality of host CdO unit cell. Hence, the structural data mentioned in Table 1 show very slight

Table 1 Structural parameters of the studies pure and Pd-doped CdO films determined by XRD; lattice parameter (a), average crystallites size (CS), texture coefficient ($TC_{(111)}$), and optical parameters: optical bandgap (E_g), Urbach parameter (E_U)

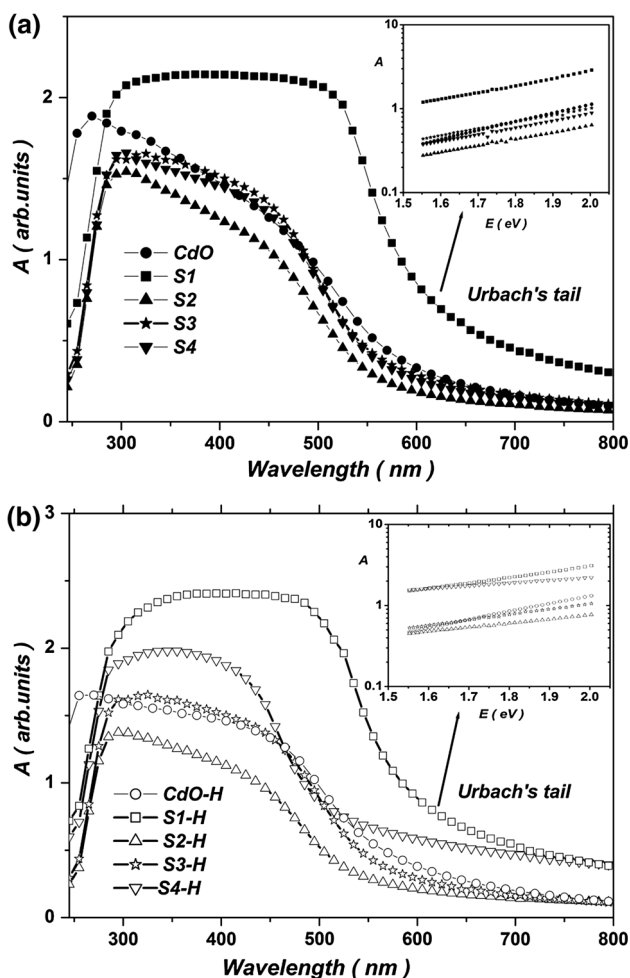| Sample	a (Å)	CS (nm)	$TC_{(111)}$	E_g (eV)	E_U (eV)
CdO	4.701	33.2	1.80	2. 18	0.47
S1	4.698	42.9	1.49	2.11	0.52
S2	4.695	34.9	3.40	2.35	0.55
S3	4.695	36.1	3.30	2.35	0.54
S4	4.695	36.3	3.18	2.32	0.53
Hydrogenation post-treatment					
CdO–H	4.672	75.8	1.53	2.28	0.44
S1-H	4.697	44.2	1.42	2.15	0.64
S2-H	4.696	31.0	~ 4.0	2.4	0.86
S3-H	4.695	36.0	3.32	2.4	0.65
S4-H	4.695	37.7	3.18	2.46	1.27

($\sim 0.1\%$) decrease of unit-cell volume of host CdO due to Pd^{2+} ionic doping. The lattice parameter was calculated from the intense (111) reflection due to the strong preferred orientation effect, and the estimated accuracy was of $\sim 10^{-3}$ Å. The little ($\sim 0.1\%$) decrease of host CdO unit-cell volume (a^3) due to Pd doping was caused by some micro stress (σ_{st}) that colud be estimated by $\sigma_{st} = \varepsilon_s B$, where B is the average bulk modulus of CdO ~ 158 GPa [27]. The average crystallite size (CS) was estimated from the most intense (111) reflection by using Scherrer's equation [28]: $CS = 0.9\lambda/\beta\cos\theta$, where λ is the X-ray wavelength (0.15406 nm); β is the full-width at half maximum (FWHM) of the (111) diffraction peak (in radian); and θ is the Bragg angle of the (111) peak. The CS values were in the interval 30–40 nm; slightly varied with Pd doping. Data of Table 1 and Fig. 1b show that the hydrogenation of pure and host CdO could not change its crystalline structure or granular nature.

3.2 Optical properties

The spectral normal transmittance $T(\lambda)$ of the prepared Pd-doped CdO films were measured in the spectral range 250–800 nm. The absorbance ($A(\lambda)$) spectra of the samples as calculated by $A(\lambda) = \ln[1/T(\lambda)]$ is shown in Fig. 2. It is clear that the main absorption region lies in the spectral range 300–500 nm, while the transparent region is being in the NIR region. The low-energy side of the spectral absorbance curves show sharp damping due to the mechanism of direct absorption edge. The optical band gap (E_g) can be evaluated by the well-known Tauc method [29]:

$$A E = A_{op} (E - E_g)^m \qquad (2)$$

where A_{op} is the film's constant and the exponent m is equal to 0.5 for direct transitions. Thus, the extrapolation of the straight-line portion of the $(AE)^2$ versus E plot, as shown in Fig. 3, gives the value of the band gap (Table 1). For undoped CdO, the bandgap obtained was in the range (2.2–2.6 eV) known for undoped CdO films prepared by different techniques [6]. Figure 4 shows graphically the variation of measured E_g with Pd% doping level. Three restrictions control the bandgap variation of the doped oxide; (1) the structural defects induced by dopant impurity that could be described by energy levels close and could merge with the bottom of the host CdO conduction band [30, 31], (2) the variation of electronic carrier concentration (N_{el}), and (3) the accumulation of H atoms on the GBs and interstitials of the crustalline structure. For low Pd% impurity concentration (sample S1), the bandgap shrank refers to the dominant effect of the first restriction, which can be confirmed by lowering of TC value (Table 1). For Pd% is larger than 3% (for samples S2, S3, and S4), the measured bandgap (E_g) was increased due to the

Fig. 2 a Spectral absorbance A(λ) of undoped and Pd-doped films. The *inset* shows Urbach plot (Log*A* vs. *E*) fitted to the experimental data points. **b** Spectral absorbance A(λ) of hydrogenated undoped and Pd-doped films. The *inset* shows Urbach plot (Log*A* vs. *E*) fitted to the experimental data points
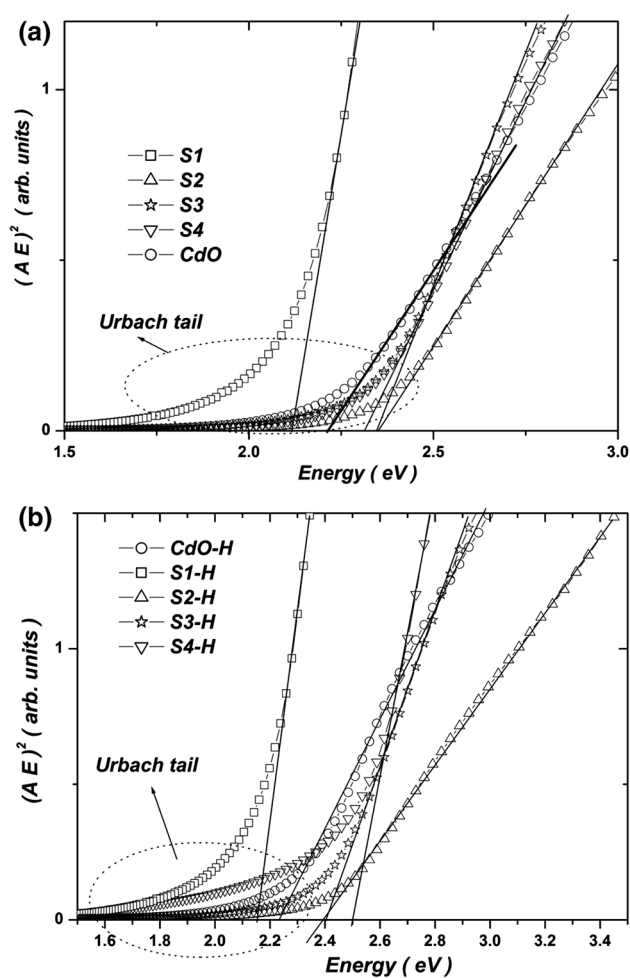

Fig. 3 a Tauc plot for undoped and Pd-doped films. **b** Tauc plot for hydrogenated undoped and Pd-doped films

improvement in the crystallinity or TC (Table 2) (there is a linear relationship between E_g and TC).

Figure 4 shows that the hydrogenation increased the bandgap of the host CdO. This can be explained by increasing of the carrier concentration (N_{el}) of samples S1-H, S2-H, and S3-H, obeying Moss-Burstein (B-M) effect [32]. However, the measured carrier concentrations (N_{el}) of the samples S3-H and S4-H are almost equal (next section) while the bandgap of sample S4-H is larger than that of S3-H. Therefore, the third restriction was the main cause that increased E_g of S4-H.

The low-energy part of the spectral absorbance shown in Fig. 2 is known as Urbach tail of the conduction band [32]. The Urbach tail of the absorption spectrum, $A(E)$ is attributed to the phonon assisted electronic transition from localised valence band states to extended conduction band states and can be analysed according to the relation: $A \sim \exp{(E/E_U)}$, where E_U is a parameter that represents
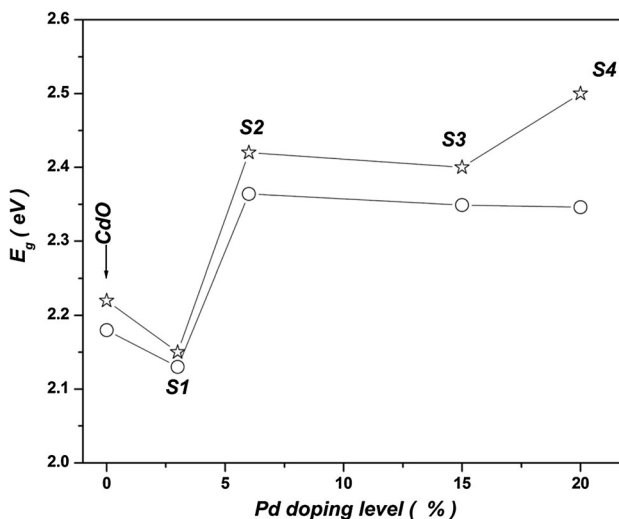

Fig. 4 Variation of bandgap with Pd % contents of undoped and Pd-doped films

**Table 2** The measured electrical parameters for hydrogenated CdO:Pd films

Sample	ρ ($\times 10^{-4}$ Ω cm)	μ_{el} (cm²/V s)	N_{el} ($\times 10^{20}$ cm⁻³)
CdO–H	69.0	8.5	1.06
S1-H	8.98	18.36	3.78
S2-H	5.16	26.75	4.52
S3-H	2.13	32.02	9.16
S4-H	6.02	11.28	9.19

the width of the exponential band tail Urbach energy and it is a measure of structural disorder. The inset of Fig. 2 illustrate the best fit of Urbach formula (Log$A$ vs. E) to the experimental data points for $E < 2.0$ eV ($\lambda > 621$ nm). The values of the parameter E_U are given in Table 1. The presence of band tail for crystalline films can be considered as a criterion to the structural inhomogeneity, defects, disorders due GBs and CBs, etc. Thus, doping of CdO increased E_U (Table 1) due to growing of host crystalline disorder. In addition, data of Table 1 demonstrate that the hydrogenation of Pd- incorporated CdO films increases their E_U parameter values. This can be attributed to the growing of disorder in the films due to increasing of density of their structural point defects (O-vacancies) by the hydrogenation. Furthermore, data of Table 1 show that the value of E_U parameter of sample S4-H (20% Pd) was significantly increased by ∼140% due to the hydrogenation. This behaviour can be attributed to a significant accumulation of dopant Pd ions on GBs in sample S4-H. Those accumulated Pd ions generate high concentration of H atoms/ions, which also accumulated on GBs, causing increase of crystalline disorder or strain and, hence, increase of E_U parameter value. Moreover, the accumulation of dopant Pd ions on GBs has great effects on the electrical properties, especially ρ and μ_{el} of S4-H in Fig. 5 (next section).

The accumulation of incorporated Pd ions on GBs of S4 sample is related to solubility limit of Pd in CdO that is estimated to be around 15%. It is useful to mention here that the solubility of Ni²⁺ ions in CdO was estimated to be ∼15% [33]

3.3 DC electrical properties

Figure 5 and Table 2 present the measured electrical conduction parameters [ρ, μ_{el} and N_{el}] of the hydrogenated Pd-doped CdO films as a function of Pd% incorporation level. The experimental error due to the size of the spot contacts in Van-der-Pauw technique was estimated to be about 5%. It can be seen that the TCO conduction parameters of host CdO films were developed with increasing of Pd% incorporation level until the sample S3-H, after which
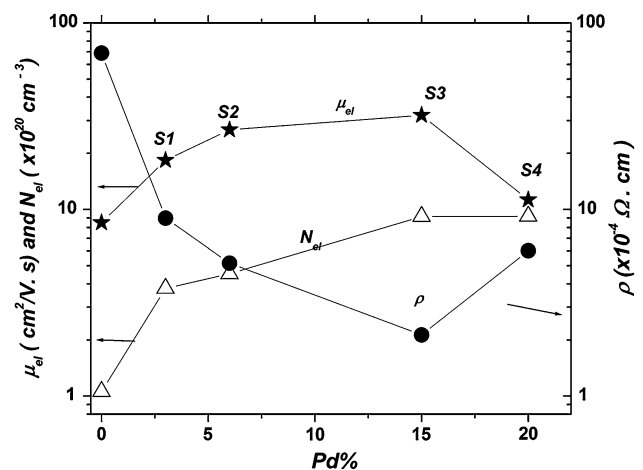
Fig. 5 Dependence of resistivity (ρ), carrier mobility (μ_{el}), and carrier concentration (N_{el}) on %Pd contents in hydrogenated Pd-doped CdO films

conduction parameters began degradation, as that for sample S4-H. This degradation is attributed to the accumulation of incorporated Pd ions (with the generated H ions) on the GBs starting from sample S3-H leading to decreasing of conductivity and carrier mobility.

Although the oxidation state of Pd (+2) is like that of Cd, the hydrogenation of samples S1, S2, and S3 increased their bandgaps due to increasing their carrier concentration, N_{el}, according to M-B effect, as shown in Fig. 4. This observation needs to be explained. In ordinary cases, annealing in H_2-gas atmosphere has usual annealing consequences, like reduction of structural defect and dislocation density. However, in case of annealing under H_2-gas atmosphere for samples incorporated with transition metal (TM) ions like in the present case, the situation is totally different. The adsorbed hydrogen H_2 molecules in host crystal lattice could be easily dissociated into H atoms/ions at presence of some transition metal (TM) dopant ions, playing a role of catalyst since the TMs are known to posses high catalytic effect for H_2 molecules dissociation [16, 17]. Then, H atoms/ions will be diffused in the host crystal lattice through interstitial sites or vacancies followed by interaction with structural oxygen forming oxygen vacancies, which interns induce/boost conduction electron concentration (N_{el}) and hence increase E_g (Fig. 4). In the present work, Pd dopant ions are considered as catalyst ions for H_2 molecule dissociation.

The factual mean-free-path (mfp) of conduction electrons can be estimated by [34]:

$$l = (h/2e)(3N_{el}/\pi)^{1/3}\mu_{el} \tag{3}$$

which gives values in the range 1–6 nm (inset of Fig. 6). The sudden decrease of the mfp in S4-H sample is due to the increase in the scattering probability of carriers at GBs

on which Pd ions and H ions (or Pd-H species) were accumulated and notably affect the measured electrical properties. That accumulation of Pd ions would enhance the carrier scattering mechanism at GBs, which cause increase in the resistivity and reduce of carrier mobility (Table 2).

The results show that the utmost enhancement of mobility (32.02 cm^2/Vs), conductivity (4.6948 × 10^3 S/cm) and carrier concentration (9.16 × 10^{20} cm^{-3}) was found with the hydrogenated CdO film doped with 15 wt% Pd.

3.4 Optoelectronic properties

Phenomenologically, to correlate the bandgap variations to the carrier concentration, both bandgap widening (BGW) and bandgap narrowing (BGN) phenomena should be considered. According to M-B model, the BGW energy is given by $BGW = S_{BGW} N_{el}^{2/3}$ [32], where $S_{BGW} = 1.348 \times 10^{-18}$ eV m^2 for host CdO [35]. The BGN energy is given by $BGN = (S_{BGN}^{(1)} N_{el}^{2/3} + S_{BGN}^{(2)} N_{el}^{1/3})$ [30, 31], where $S_{BGN}^{(1)} = 4.49 \times 10^{-19}$ eV m^2, $S_{BGN}^{(2)} = 2.836 \times 10^{-9}/\varepsilon_r$ eV m^2, and ε_r is the effective dielectric constant host CdO [35]. Thus, the change in bandgap ($\Delta E_g = E_g - E_g^0$) is given by:

$$\Delta E_g = (BGW - BGN)$$
$$= S_{BGW,BGN} N_{el}^{2/3} - S_{BGN}^{(2)} N_{el}^{1/3} + C_f \quad (4)$$

where C_f is a fitting parameter and $S_{BGW,BGN} = S_{BGW} - S_{BGN}^{(1)} = 8.98 \times 10^{-19}$ eV m^2. Therefore, a straight line should be obtained by plotting optoelectronic function
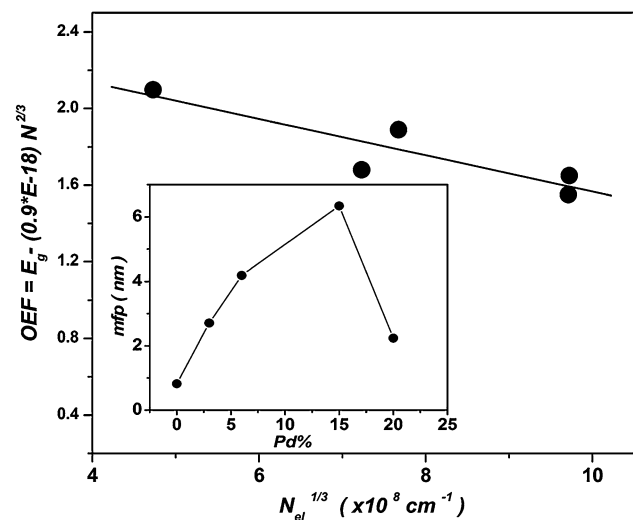

Fig. 6 Optoelectronic function plot: OEF = $[E_g - S_{BGW,BGN} N_{el}^{2/3}]$ versus $N_{el}^{1/3}$. The *inset* is the %Pd-content function of mean free path (mfp)

OEF = $[E_g - S_{BGW,BGN} N_{el}^{2/3}]$ versus $N_{el}^{1/3}$, as shown in Fig. 6, where $S_{BGN}^{(2)} = 9.47 \times 10^{-10}$ eV m^2. With $\varepsilon_r = n^2 = 3$ (where n ~ 1.73 is the average refractive index of CdO at transparent region [36]), the experimental and theoretical values of $S_{BGN}^{(2)}$ are almost identical that shows fine description.

4 Conclusions

The present work shows that it is possible to prepare Pd-and H-codoped CdO thin films. The structural results showed that doping with Pd ions strongly enhanced the [111] preferred orientation growth, especially at doping level around 6% with hydrogenation. The utmost enhancement of mobility (32.02 cm^2/Vs), conductivity (4.6948 × 10^3 S/cm) and carrier concentration (9.16 × 10^{20} cm^{-3}) was found with the hydrogenated CdO film doped with 15 wt% Pd. These results confirm the possibility of using CdO:Pd-H films in TCO applications, with high carrier concentration ~10^{21} m^{-3}.

References

1. Y. Dou, R.G. Egdell, T. Walker, D.S.L. Law, G. Beamson, Surf. Sci. **398**, 241 (1998)
2. B.J. Lewis, D.C. Paine, Mater. Res. Soc. Bull. **25**, 22 (2000)
3. M. Yan, M. Lane, C.R. Kannewurf, R.P.H. Chang, Appl. Phys. Lett. **78**, 02342 (2001)
4. D.M. Carballeda-Galicia, R. Castanedo-Perez, O. Jimenez-Sandoval, S. Jimenez-Sandoval, G. Torres-Delgado, C.I. Zuniga-Romero, Thin Solid Films **371**, 105 (2000)
5. Powder Diffraction File, Joint Committee for Powder Diffraction Studies (JCPDS) file No. 05-0640
6. Z. Zhao, D.L. Morel, C.S. Ferekides, Thin Solid Films **413**, 203 (2002)
7. O.G. Daza, A.A.-C. Readigos, J. Campos, M.T.S. Nair, P.K. Nair, Mod. Phys. Lett. B **17**, 609 (2001)
8. P.K. Gupta, K. Ghosh, R. Patel, S.R. Mishra, P.K. Kahol, Curr. Appl. Phys. **9**, 673 (2009)
9. S. Shu, Y. Yang, J.E. Medvedova, J.R. Ireland, A.W. Metz, J. Ni, C.R. Kannewurf, A.J. Freeman, T.J. Tobin, J. Am. Chem. Soc. **126**(2004), 13787 (2004)
10. A.A. Dakhel, Thin Solid Films **518**, 1712 (2010)
11. A.A. Dakhel, J. Alloys Compd. **475**, 51 (2009)
12. R.D. Shannon, Act Crystallogr. A **32**, 751 (1976)
13. A.A. Dakhel, Adv. OptoElectron. (2013). doi:10.1155/2013/804646
14. A.A. Dakhel, J. Electron. Mater. **41**, 2405 (2012)
15. R.K. Gupta, F. Yakuphanoglu, F.M. Amanullah, Phys. E **43**, 1666 (2011)
16. E.A. Lewis, D. Le, C.J. Murphy, A.D. Jewell, M.F.G. Mattewra, M.L. Liriano, T.S. Rahman, E.C.H. Sykes, J. Phys. Chem. C **116**, 25868 (2012)
17. M. Pozzo, D. Alfe, Int. J. Hydrog. Energy **34**, 1922 (2009)
18. Y. Ghayeb, M.M. Momeni, A. Mozafari, J. Mater. Sci.: Mater. Electron. **27**, 11804 (2016)

19. M.M. Momeni, Z. Nazari, Ceram. Int. **42**, 8691 (2016)
20. N. Güy, S. Çakar, M. Özacar, J. Colloid Interface Sci. **466**, 128 (2016)
21. J. Ma, Y. Liu, H. Zhang, P. Ai, N. Gong, Y. Zhang, Nanoscale Res. Lett. **9**, 503 (2014)
22. L. Chen, X. He, Y. Liang, Y. Sun, Z. Zhao, H. Jie, J. Mater. Sci.: Mater. Electron. (2016). doi:10.1007/s10854-016-5257-z
23. S.M. Sze, *Semiconductor Devices, Physics and Technology* (Bell Telephone Laboratories Inc., Whippany, 1985)
24. A.A. Dakhel, H. Hamad, Int. J. Thin Film Sci. Technol. **1**, 25 (2012)
25. C.S. Barrett, T.B. Massalski, *Structure of Metals* (Pergamon, Oxford, 1980), p. 204
26. C. Kittel, *Introduction to Solid State Physics*, 7th edn. (Wiley, New York, 1996)
27. H. Liu, H.-K. Mao, M. Somayazulu, Y. Ding, Y. meng, D. Hausermann, Phys. Rev. B **70**, 094110 (2004)
28. E.F. Kaelble (ed.), *Handbook of X-rays for Diffraction, Emission, Absorption, and Microscopy* (McGraw-Hill, New York, 1967), p. 17
29. J. Tauc, F. Abelesn (eds.), *Optical Properties of Solids* (North Holland, Amsterdam, 1969)
30. Y.Z. Zhang, J.G. Lu, Z.Z. Ye, H.P. He, L.P. Zhu, B.H. Zhao, L. Wang, Appl. Surf. Sci. **254**, 1993 (2008)
31. W. Walukiewicz, Phys. Rev. B **41**, 10218 (1990)
32. J.I. Pankove, *Optical Progress in Semiconductors* (Dover Publications, New York, 1975)
33. T. Ahmed, S. Khatoon, K. Coolahan, S. Lofland, J. Mater. Res. **28**, 1245 (2013)
34. E.H. Sondheimer, Adv. Phys. **1**, 1 (1952)
35. A.A. Dakhel, Curr. Appl. Phys. **11**, 11 (2011)
36. K. Gurumurugan, D. Mangalaraj, S.K. Narayandass, K. Sekar, C.P. Girija Vallabhan, Semicond. Sci. Technol. **9**, 1827 (1994)